JOURNAL OF MECHANICS OF CONTINUA AND MATHEMATICAL SCIENCES
www.journalimcms.org

ISSN (Online) : 2454 -7190 Vol.-20, No.-5, May (2025) pp 112 - 133 ISSN (Print) 0973-8975

DYNAMICS OF CHOLERA TRANSMISSION: A MATHEMATICAL MODELING FRAMEWORK FOR ANALYZING EPIDEMIC PROPAGATION

W. Sukpol[1], P. Pornphol[2], P. Hammachukiattikul[3], S. Emmanuel[4] S. Sathasivam[5]

[1,3] Department of Mathematics, Faculty of Science and Technology, Phuket Rajabhat University, Phuket 83000, Thailand.

[2]Department of Digital Technology, Faculty of Science and Technology, Phuket Rajabhat University, Phuket 83000, Thailand.

[4]Department of Mathematics, Faculty of Science, Lokoja-Nigeria.

[5] School of Mathematical Sciences, Universiti Sains Malaysia, 11800 USM Pulau Pinang, Malaysia.

[1]wimonnat.s@pkru.ac.th, [2]putsadee.p@pkru.ac.th, [3]porpattama@pkru.ac.th
[4]sabastine.emmanuel@fulokoja.edu.ng, [5]saratha@usm.my

Corresponding Author: **Saratha Sathasivam**

https://doi.org/10.26782/jmcms.2025.05.00009

(Received: March 05, 2025; Revised: April 28, 2025; Accepted: May 09, 2025)

Abstract

Cholera remains a significant public health concern globally, offering an opportunity to construct robust transmission models that elucidate its dynamics and guide intervention strategies. In this study, we develop a refined cholera transmission model that accounts for time-dependent recovery rates and persistent environmental reservoirs, extending beyond the assumptions of traditional SIR-type frameworks. The model segments the population into compartments—susceptible, infected, and statistical storage of relevant variables—allowing for dynamic epidemic progression under specified parameter values. Historical data on cholera cases, fatalities, and case-fatality rates spanning multiple years underwent rigorous preprocessing, including linear interpolation, to ensure robustness. We employed a least-squares curve-fitting approach to estimate key parameters, which optimizes model accuracy and allows simulation of disease progression and intervention effectiveness over time. Results from our model yield critical insights into cholera transmission, including the roles of environmental bacterial reservoirs and drug treatments in moderating infection rates. These estimated parameters provide policymakers with actionable data for designing targeted interventions, enhancing public health responses, and mitigating cholera's impact on vulnerable populations. This work emphasizes the value of mathematical modeling as a tool for understanding infectious disease dynamics and developing strategies to reduce epidemic impacts.

Keywords: Cholera, Curve Fitting, Numerical Simulation, Seasonal Outbreak, Transmission dynamics.

I. Introduction

Cholera is a highly infectious disease caused by the bacterium Vibrio cholerae. It is usually spread from person to person through contaminated food and drinking water. As an infectious disease, cholera still ranks as one of the major public health problems in many developing countries, especially where clean drinking water and proper sanitation are unavailable. According to the World Health Organisation [X], cholera affects millions of people each year, the world over. The symptoms are severe, and death rates are also one of the 1st biggest killers among infants. The persistence of the cholera outbreak demands efforts in prevention and control programs that are effective at minimizing its effects on vulnerable populations.

Cholera epidemics are influenced by a confluence of environmental, social, and infrastructural conditions that facilitate the dissemination of the pathogen Vibrio cholerae [II-IV]. The following drivers are included: Cholera is predominantly spread by contaminated water and food, rendering communities with inadequate access to clean water and sanitation facilities highly susceptible to infection. Insufficient sewage disposal systems, the absence of chlorination in water sources, and substandard hygiene standards can all promote the transmission of cholera. Floods, particularly during monsoon seasons, can inundate existing infrastructure, polluting drinking water with sewage and heightening the danger of epidemics, as discussed by [XVI]. Cholera outbreaks frequently demonstrate seasonal trends, with an increase in incidence during warmer months or following substantial rainfall [IX, XVI, XVII]. Elevated temperatures and humidity can facilitate the proliferation of Vibrio cholerae in coastal waters, but variations in water pH and salinity can influence bacterial viability. Bacteria are frequently linked to phytoplankton and zooplankton blooms, which may intensify under warmer temperatures, facilitating bacterial multiplication, as discussed by [X, XXI]. Population Density: Accelerated, unregulated urbanization in low-income areas can result in congested habitats with insufficient water and sanitation infrastructure, fostering optimal circumstances for cholera epidemics. Elevated population density exacerbates transmission risk and complicates the implementation of effective containment strategies.

In areas with inadequate healthcare resources, the detection and management of cholera outbreaks can be challenging. The absence of skilled healthcare professionals, swift diagnostic instruments, and effective public health surveillance systems might hinder outbreak response, permitting cholera to proliferate before measures are enacted by [XVII]. Migration and Displacement caused by conflict, natural disasters, or economic adversity can lead to substantial populations residing in temporary encampments or urban slums, frequently lacking sufficient sanitation and healthcare services [V]. These conditions engender significant susceptibility to waterborne infections such as cholera, as evidenced by recent outbreaks in refugee camps in South Sudan and Bangladesh.

When it comes to understanding and controlling infectious diseases, mathematical models have played a crucial role in public health. By depicting the dynamics of disease dissemination through susceptible, infectious, and recovered compartments, [VII, XII, XIII, XV] use stochastic and deterministic mathematical models of cholera disease dynamics with direct transmission. [VI] and other recent research have broadened this approach to incorporate compartments such as exposed, vaccinated, and quarantined. Predicting infection rates and directing interventions such as lockdowns and vaccinations were made possible by mathematical models throughout the COVID-19 pandemic [VII, XIX].

Mathematical models find extensive use in environmental systems to predict the effects of climate change, manage resources, and understand the dynamics of pollutants. For example, [XX] discussed modeling the influence of environmental pollution on waterborne diseases. Sustainable development strategies and mitigation measures can be better crafted with the use of these models. Mathematical models play a vital role in understanding the spread of infectious diseases like cholera, enabling researchers to track transmission patterns, forecast outbreaks, and assess the impact of control measures [I]. Strategic decision-making by health authorities and community responses, such as water sanitation practices and vaccination campaigns, have been explored using models developed by [VI-VIII]. Models inspired by the work of [XX, XIV] also highlight how environmental improvements contribute to sustained public health and economic resilience in cholera-prone areas. Moreover, mathematical modeling supports the efficient design and optimization of sanitation and water purification systems. The flow of contaminated water through river systems, a key factor in cholera transmission, is analyzed using differential equations [XV].

Previous studies used different mathematical frameworks to uncover all the environmental interactions between human populations that lead to cholera outbreaks. For example, [III] developed a compartment model to represent these dynamics and found that the concentration of bacteria in the environment had a significant impact on the transmission of cholera. In addition, [VI, XII] used a Susceptible-Infectious-Recovered (SIR) model to judge how effective vaccination strategies would be. The findings showed that there may be some limited channels in reducing cholera incidence through intervention. While models of cholera have grown in sophistication over the years, certain key parameters governing disease transmission are still difficult to estimate precisely. The traditional approach is almost always used, with limited data sets causing parameters to be estimated imprecisely. Also, the interplay between environmental conditions, human behavior, and the intrinsic growth rate of Vibrio cholerae makes modeling more complex. As a result, there is an urgent need for comprehensive models that embrace these complexities so that our understanding of cholera dynamics improves. To accomplish the goal of performing a numerical simulation of the cholera pandemic, the Runge-Kutta 4th Order (RK4) method will be utilized. This will make it possible to arrive at a more precise estimation of the dynamics of the model, as well as to conduct a more straightforward investigation of crucial factors, such as time-dependent transmission rates and how they influence the advancement of the epidemic. This supplement strengthens the study and assures the

right findings when checking and evaluating the models by paying attention to the methodological rigor that is required to solve challenging nonlinear systems. Therefore, the study is strengthened and guarantees proper findings.

In this study, we aim to develop a mathematical framework for cholera dynamics that incorporates disease-induced mortality and environmental factors. The objectives of this research are: (1) to establish a compartmental model for cholera infection dynamics representing the susceptible, infected, and recovered populations; (2) to take into account the impact of environmental bacterial concentrations on transmission dynamics; (3) through a curve-fitting technique, to estimate key parameters governing cholera dynamics from historical case data, and (4) use the estimated parameters to simulate cholera transmission dynamics and judge how effective different intervention strategies are for varying levels of incidence. By attaining these objectives, this study will provide a deeper understanding of cholera dynamics and will offer public health policymakers valuable insights to guide their efforts at curbing cholera outbreaks.

II. Mathematical Model

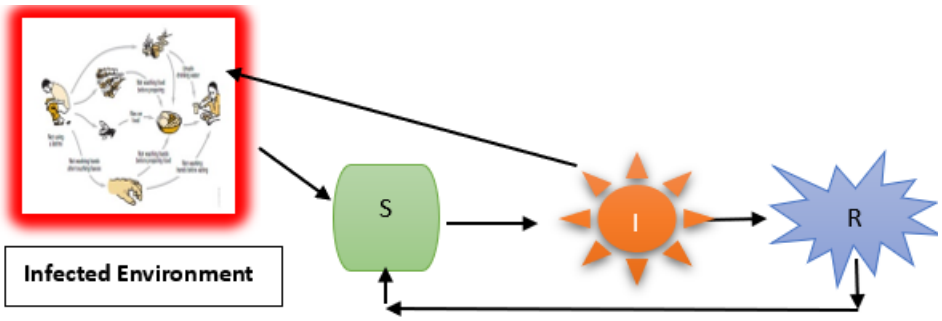

Fig. 1: Diagrammatic representation of the model

Variables

$S(t)$: Susceptible individuals at times t

$I(t)$: Infected individuals at the time t

$R(t)$: Recovered individuals at the time t

$B(t)$: The concentration of cholera bacteria in the environment at the time t

$N(t)$: Total population at the time t, which is now dynamic and given by:

$$N(t) = S(t) + I(t) + R(t) \tag{1}$$

Parameters

β: Environment-to-human transmission rate (infection from contaminated water)/Time-dependent transmission rate from bacteria in the environment

α: Human-to-human transmission rate (Time-dependent transmission rate from infected individuals)

κ: Carrying capacity for the bacteria in the environment

w: Rate of water sanitation or environmental cleanup

μ: Natural birth rate and natural death rate (assumed to be equal)

ξ: Human-to-environment transmission rate (bacterial shedding by infected individuals)

r: Intrinsic growth rate of cholera bacteria

γ: Natural bacterial death rate

a: Recovery rate due to treatment

δ: Disease-induced death rate for infected individuals

d: Death rate due to cholera

Population dynamics

Susceptible population: The susceptible individuals' population rises due to births and declines due to illnesses, natural mortality, and immunization.

$$s' = \mu\text{-}(\alpha I + \beta B)S\text{-}\mu S\text{-}vS \quad (2)$$

Infected Population Dynamics: The infected population rises from new infections and declines owing to mortality from the disease, recoveries from therapy, and natural deaths:

$$I' = (\alpha I + \beta B)S\text{-}(\mu + \delta + a + d)I \quad (3)$$

$(\alpha I + \beta B)S$: The transmission of new infections through contact with infected individuals and contaminated environments.

$(\mu + \delta)I$: Loss of infected individuals due to natural death μ and disease-induced death δ and αI: Recoveries due to treatment.

Recovered Population Dynamics: Recovered individuals increase due to treatment and vaccination and decrease due to natural death**.**

$$R' = aI + vS\text{-}\mu R \quad (4)$$

Where

αI: Recoveries due to treatment of infected individuals, vS: Individuals vaccinated from the susceptible class, and μR: Natural death of recovered individuals

Bacteria population dynamics

Shredding from infected individuals facilitates the growth of the bacterial population, while environmental factors constrain this growth. Sanitation initiatives decrease the bacterial load.

$$B' = \xi I + rB(1-B/k) - \gamma B - wB \quad (5)$$

Here:

ξ: Bacteria are shed by infected individuals, $rB(1 - B/k)$: Logistic growth of the bacteria, constrained by the carrying capacity κ, γB: Natural death of bacteria, and wB: Bacteria are removed through sanitation efforts.

Total Population Dynamics: The total population is now dynamic, accounting for births and deaths (both natural and disease-induced):

$$\frac{dN}{dt} = \mu - \delta I \quad (6)$$

μ: Births add new individuals to the population and δI Disease-induced deaths reduce the total population. With the non-negative initial conditions

Time-dependent transmission rates:

The dynamics of infectious diseases are inherently complex, with transmission rates often influenced by a range of time-dependent factors. Traditional models commonly assume a constant transmission rate; however, in reality, transmission rates can fluctuate due to seasonal variations, changes in population behavior, environmental factors, or intervention strategies. Accounting for these temporal variations is essential for accurately modeling disease spread and understanding epidemic patterns. In this study, we explore the concept of time-dependent transmission rates, incorporating these fluctuations into mathematical models to better capture the nuanced transmission dynamics of infectious diseases. By employing time-varying parameters, we aim to improve the predictive accuracy of disease models and provide a more realistic framework for assessing potential interventions, forecasting outbreak trajectories, and informing public health responses. This approach highlights the need to move beyond static models, embracing dynamic frameworks that align more closely with real-world epidemiological processes.

$$\alpha(t) = \alpha_0 \left(1 + A_\alpha sin\left(\frac{2\pi t}{T}\right)\right) \quad (7)$$

$$\beta(t) = \beta_0 \left(1 + A_\beta sin\left(\frac{2\pi t}{T}\right)\right) \quad (8)$$

Where

α_0: Baseline human-to-human transmission rate, $\boldsymbol{A_\alpha}$: Amplitude of seasonal variation for $\alpha(t)$, $\boldsymbol{A_\beta}$: Amplitude of seasonal variation for $\beta(t)$ and T: Period of seasonal variation (typically 365 days for yearly cycles). The transmission rates $\alpha(t)$ and $\beta(t)$ vary with time to account for seasonal effects. These are modeled as sinusoidal functions:

$$S(0) \geq 0, I(0) \geq 0, B(0) \geq 0, R(0) \geq 0 \quad (9)$$

At the Disease-Free Equilibrium (DFE), there are no ill individuals $(I = 0)$ and no bacteria are present in the environment $(B = 0)$. The sensitive population(S)maintains its equilibrium value, whereas the recovered population (R)

is either nonexistent or at a steady state. At the DFE, the population is entirely susceptible, so the number of susceptible individuals is at its maximum. The population is completely susceptible at the DFE, which means that the number of vulnerable persons is at its highest point. Therefore $S = S_0$, also where S_0 is the total population at equilibrium. Since the population size is often assumed constant in epidemiological models, we consider:

$$S_0 + R_0 = N^* \tag{10}$$

The disease-free equilibrium point is thus:

$$(S_0, I_0, R_0, B_0) = (S_0, 0,0,0) \tag{11}$$

$$\frac{dI}{dt} = \alpha_0 S_0 I + \beta_0 S_0 I - (\mu + \delta + a + d)I \tag{12}$$

$$\frac{dB}{dt} = \xi \mathrm{I} - \gamma \mathrm{B} - \mathrm{wB} \tag{13}$$

$$F = \begin{pmatrix} \alpha_0 S_0 & \beta_0 S_0 \\ 0 & 0 \end{pmatrix} \tag{14}$$

New infections in I (infected individuals) are caused by direct transmission from infected individuals α_0 and environmental transmission from bacteria β_0. The second row is the bacteria equation, where no new illnesses influence bacteria.

$$V = \begin{pmatrix} \mu + \delta + a + d & 0 \\ -\xi & \gamma + \mathrm{w} \end{pmatrix} \tag{15}$$

$$FV^{-1} = \begin{pmatrix} \alpha_0 S_0 & \beta_0 S_0 \\ 0 & 0 \end{pmatrix} \begin{pmatrix} \frac{1}{\mu+\delta+a+d} & 0 \\ \frac{\xi}{(\mu+\delta+a+d)(\gamma+\mathrm{w})} & \frac{1}{\gamma+\mathrm{w}} \end{pmatrix} \tag{16}$$

Simplifying, the dominant eigenvalue (trace of the matrix) gives us

$$R_0 = \frac{\alpha_0 S_0}{\mu+\delta+a+d} + \frac{\beta_0 S_0 \xi}{(\mu+\delta+a+d)(\gamma+\mathrm{w})} \tag{17}$$

$\frac{\alpha_0 S_0}{\mu+\delta+a+d}$: The number of secondary infections caused by direct transmission from infected individuals.

$\frac{\beta_0 S_0 \xi}{(\mu+\delta+a+d)(\gamma+\mathrm{w})}$: The number of secondary infections caused by environmental transmission from bacteria.

We calculate the fundamental reproduction number R_0 to assess disease spread potential, starting with baseline transmission rates α and β. These metrics describe average transmission rates without seasonal changes.

At the DFE, we substitute $I = 0$ and $B = 0$ into these equations. This will enable us to linearise the system around the DFE. The linearised system for I and B is as follows:

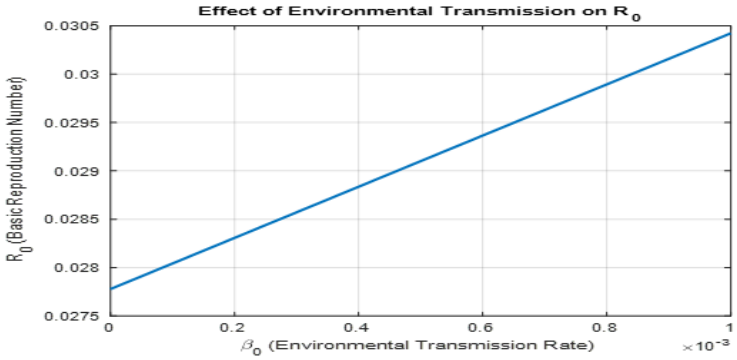

Fig. 2. Diagrammatic representation of the effect of environmental transmission on R_0

The graph in Figure 2 illustrates the relationship between the basic reproduction number R_0, and the environmental transmission rate β_0, highlighting the influence of environmental factors on disease spread. The basic reproduction number R_0, is a key epidemiological metric representing the average number of secondary cases generated by one infectious individual in a fully susceptible population. It provides critical insight into the transmission potential of an infectious disease and the likelihood of an outbreak within a population. In this model, R_0 demonstrates a linear increase with rising values of β_0, indicating that higher environmental transmission rates directly enhance the reproduction number. The parameter β_0 reflects the efficiency of pathogen transmission via environmental reservoirs, such as water sources contaminated with cholera bacteria. A linear relationship suggests that as β_0 increases signifying greater environmental bacterial concentration and contamination—there is a proportional rise in R_0 which implies a higher risk of disease spread within the community.

This linearity underscores the significance of managing environmental contamination to mitigate disease transmission. Specifically, reducing β_0 through strategies aimed at lowering bacterial shedding into the environment, could proportionally decreaseR_0, thereby reducing the likelihood of an outbreak. This insight emphasizes the importance of environmental control measures, such as improved sanitation and water treatment, in preventing cholera transmission. By addressing these environmental parameters, public health strategies can achieve a critical reduction in β_0 helping to control and prevent cholera epidemics in susceptible populations.

III. Application of the Runge-Kutta method

It is common knowledge that the Runge-Kutta methods are among the most effective numerical approaches for solving ordinary differential equations with given initial values. These methods are utilized in the fields of computer mathematics and numerical analysis. As a result of the fact that it strikes a compromise between accuracy and computational efficiency, the fourth-order Runge-Kutta method (RK4) is one of the predominant approaches among them. When it comes to approximation solutions to ordinary differential equations (ODEs) that cannot be solved analytically, these methods are crucial since they provide a pathway for solutions through numerical integration. When using the traditional RK4 approach, it is necessary to

determine the slope at four different sites inside each step interval. The general form of this algorithm is presented below.

This iterative scheme ensures higher accuracy compared to simpler methods like the Euler method, particularly for solving compartmental models where systems of ODEs describe the dynamics of various interacting populations or substances. In this study, the RK4 method was applied to solve the cholera model, treating each equation in the system as an individual ODE. The compartments—susceptible, infected, recovered, and bacteria concentrations—were updated iteratively using RK4 formulas. Initial values were specified, and a step size (h) was selected to balance accuracy and computational cost. The numerical solutions obtained for the model variables were analyzed to understand disease transmission dynamics and the effects of key parameters such as transmission rates (α,β) and recovery rate (ξ).

The application of the RK4 method provided precise approximations of the cholera model's dynamics, as evidenced by the resulting plots, which effectively illustrated the system's behavior

under different parameter settings and initial conditions. This underscores the RK4 method's robustness and reliability for solving complex nonlinear ODE systems.

$$k_{1,s} = \mathrm{h}(\mu\text{-}(\alpha(\mathrm{t_n})\mathrm{I_n} + \beta(\mathrm{t_n})\mathrm{B_n})\mathrm{S_n}\text{-}\mu\mathrm{S_n}\text{-}\nu\mathrm{S_n}) \tag{18}$$

$$k_{2,s} = \mathrm{h}\left[\left(\mu\text{-}\left(\alpha(\mathrm{t_n}+\frac{\mathrm{h}}{2})\mathrm{I_n} + \beta(\mathrm{t_n}+\frac{\mathrm{h}}{2})\mathrm{B_n}\right)\left(\mathrm{S_n}+\frac{\mathrm{k_{1,s}}}{2}\right)\text{-}\mu\left(\mathrm{S_n}+\frac{\mathrm{k_{1,s}}}{2}\right)\text{-}\nu\left(\mathrm{S_n} + \frac{\mathrm{k_{1,s}}}{2}\right)\right)\right]$$

Then compute $k_{3,s}$ and $k_{4,s}$ before updating

$$S_{n+1} = \frac{1}{6}\left[k_{1,s} + 2k_{2,s} + 2k_{3,s} + k_{4,s}\right] \tag{19}$$

The same RK4 procedure applies to the equations for I(t), R(t), and B(t), using their respective differential equations.

$$\begin{aligned} k_{1,I} &= \mathrm{h}[(\alpha(\mathrm{t_n})\mathrm{I_n} + \beta(\mathrm{t_n})\mathrm{B_n})\mathrm{S_n}\text{-}(\mu + \delta + \mathrm{a} + \mathrm{d})\mathrm{I}] \\ k_{1,R} &= h[\boldsymbol{\nu S} + \boldsymbol{aI} - \boldsymbol{\mu R}] \\ k_{1,B} &= h\left[\boldsymbol{\xi I} + \boldsymbol{rB}\left(\mathbf{1} - \frac{\boldsymbol{B}}{\boldsymbol{k}}\right) - (\gamma + w)B\right] \end{aligned} \tag{20}$$

After calculating K_1, K_2, K_3, K_4 for each compartment, update the variables iteratively.

This process is repeated over a predefined time, and the compartments are evaluated at each time step to simulate the cholera dynamics under given parameters

Algorithm/Flow Chart: RK4 Method for Cholera Model

1. **Initialization**:
    - Define the initial conditions
    - $S(0), I(0), R(0), B(0) S(0), I(0), R(0), B(0).$
    - Set the time step h and the total simulation time T_{end}.
    - Define the parameters $\alpha_0, \beta_0, A_\alpha, A_\beta, \mu, v, \delta, a, d, \xi, r, \kappa, \gamma, w$
2. **Time-Dependent Transmission Rates**: For each time t, compute:

$$\alpha(t) = \alpha_0(1 + A_\alpha sin(2\pi t/T))$$

$$\beta(t) = \beta_0(1 + A_\beta sin(2\pi t/T))$$

3. **Iterative Loop**:
    - For $t = 0$ to T_{end} with step h:

Compute RK4 Coefficients for S, I, R, BS, I, R, B:

$\mathrm{k_{1,S}} = \mathrm{h} \cdot \mathrm{f_S}(\mathrm{t_n}, \mathrm{S_n}, \mathrm{I_n}, \mathrm{R_n}, \mathrm{B_n})$

$\mathrm{k_{1,I}} = \mathrm{h} \cdot \mathrm{f_I}(\mathrm{t_n}, \mathrm{S_n}, \mathrm{I_n}, \mathrm{R_n}, \mathrm{B_n})$

$\mathrm{k_{1,R}} = \mathrm{h} \cdot \mathrm{f_R}(\mathrm{t_n}, \mathrm{S_n}, \mathrm{I_n}, \mathrm{R_n}, \mathrm{B_n})$

$\mathrm{k_{1,S}} = \mathrm{h} \cdot \mathrm{f_B}(\mathrm{t_n}, \mathrm{S_n}, \mathrm{I_n}, \mathrm{R_n}, \mathrm{B_n})$

Repeat for K_2, K_3, K_4 using updated arguments:

$$k_{2,S} = h \cdot f_S\left(t_n + \frac{h}{2}, S_n + \frac{k_{1,S}}{2}, I_n + \frac{k_{1,I}}{2}, R_n + \frac{k_{1,R}}{2}, B_n + \frac{k_{1,B}}{2}\right)$$

Similar update for k_3 and k_4

Update State Variables:

$$S_{n+1} = S_n + \frac{1}{6}\left(k_{1,S} + 2k_{2,S} + 2k_{3,S} + k_{4,S}\right)$$

$$I_{n+1} = I_n + \frac{1}{6}\left(k_{1,I} + 2k_{2,I} + 2k_{3,I} + k_{4,I}\right)$$

Similar updates for R_{n+1} and B_{n+1}.

1. **Store Results**: Save S, I, R, B for each time step t
2. **Post-Processing**:
    - Plot $S(t), I(t), R(t), B(t)$ over time.
    - Analyze the impact of parameters α, β, ξ on the dynamics.

This algorithm and the flow chart below provide a framework for implementing the RK4 method to numerically simulate the cholera model and study the influence of time-dependent transmission rates.

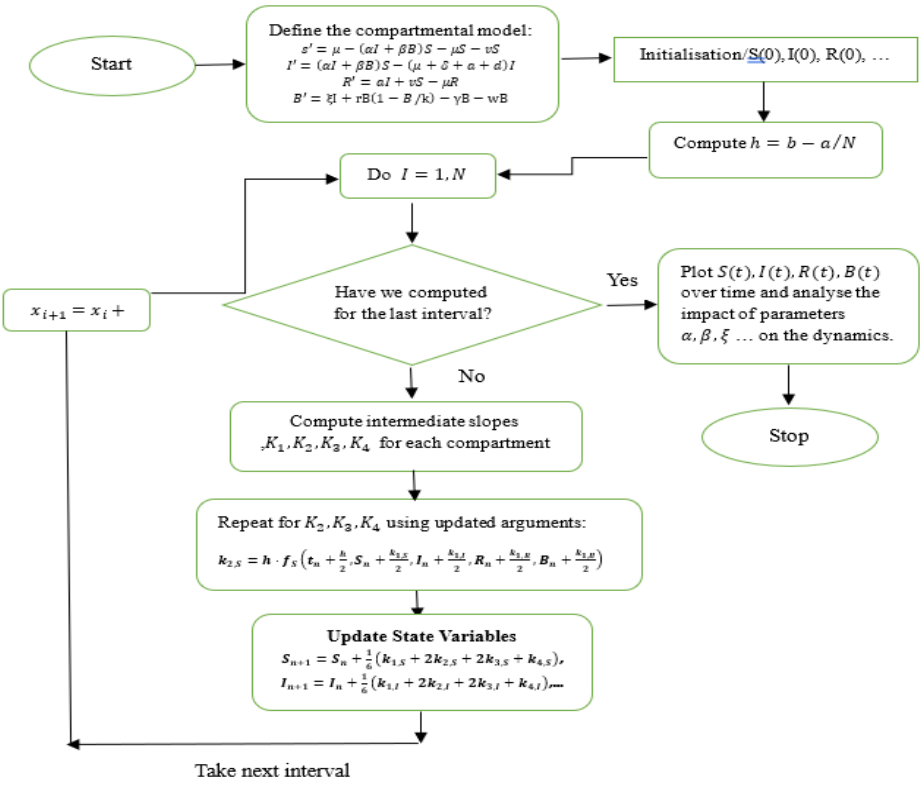

Fig. 3. Flowchart illustrating the application of the RK4 method

IV. Data Collection, Simulation, and Results

The dataset used in this analysis, derived from [III], presents a comprehensive record of cholera cases, deaths, and associated epidemiological trends over a specified period. This dataset provides essential insight into the transmission dynamics of cholera, capturing temporal patterns in infection incidence and case-fatality rates. Leveraging these historical data, we could parameterize the disease transmission model effectively, with parameter estimation detailed in Figure 3. By integrating these empirical observations, the model enables a more nuanced depiction of cholera outbreaks, capturing both infection propagation and mortality outcomes. The model further accounts for key drivers of transmission, including seasonality, population movement, and environmental bacterial loads, which are instrumental in shaping the course of an outbreak. Consequently, this refined model enhances our understanding of cholera epidemiology by enabling precise simulation of outbreak scenarios and the impact of intervention strategies, thereby supporting more informed public health**.**

V. Parameter Estimation Methodology

To calibrate the cholera transmission model and estimate unknown parameters (e.g., transmission rate β, recovery rate ξ, mortality rate d), we employed

the nonlinear least squares curve-fitting approach using MATLAB's lsqcurvefit function. This method minimizes the objective function defined as follows:

$$J(\theta) = \sum_{i=1}^{n}[y_{obs}(t_i) - y_{model}(t_i, \theta)]^2 \quad (21)$$

$$\text{Case Fatality Rate } (CFR(t_i)) = \frac{Deaths(t_i)}{Infected(t_i)} \times 100 \quad (22)$$

Where $J(\theta)$ is the objective function, $y_{obs}(t_i)$ the observed cholera case or death data from time t_i, $y_{model}(t_i, \theta)$ is the model-predicted output with the parameter vector θ, θ is the vector of unknown parameters to be estimated, n is the number of data points (years or months, depending on resolution). Also, an exponential model with two terms can be used to fit the case data $C(t) = a_1 e^{b_1 t} + a_2 e^{b_2 t}$ and $D(t) = C_1 e^{d_1 t} + C_2 e^{d_2 t}$, $C(t)$ and $D(t)$ number of cholera and death cases at a time t.

Due to gaps in certain years, linear interpolation was applied to reconstruct missing points. For missing data at year t, where the known data values are at t_n and t_{n+1} with $(t_n < t < t_{n+1})$

$$y(t) = y(t_n) + \frac{y(t_{n+1}) - y(t_n)}{t_{n+1} - t_n} \times (t - t_n) \quad (23)$$

Here, $y(t)$ is the interpolated value, $y(t_{n+1}), y(t_n)$ are the known data values before and after the missing year?

A simple moving average was computed to smooth the data and reduce noise. This equation is given as

$$y_{smooth} = \frac{1}{3}(y(t-1) + y(t) + y(t+1)) \quad (24)$$

The data values for the previous, current, and next years are $y(t-1), y(t)$ and $y(t+1)$ respectively.

Model validation was carried out by cross-validating the dataset and assessing prediction accuracy using the Root Mean Squared Error (RMSE) as the goodness-of-fit metric.

$$RMSE = \sqrt{\frac{1}{n}\sum_{i=1}^{n}[y_{obs}(t_i) - y_{model}(t_i, \theta)]^2} \quad (25)$$

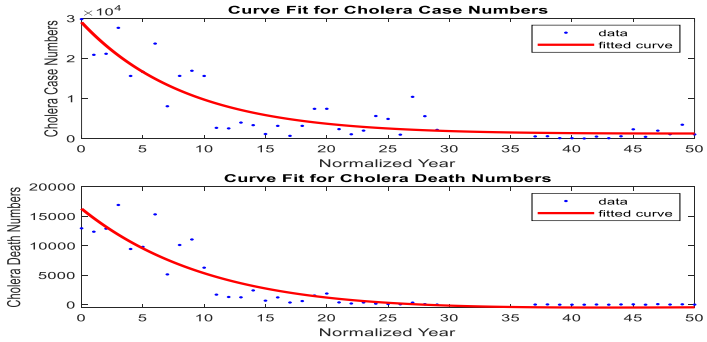

Fig. 4. Curve fit for cholera and death cases.

Figure 3: Top Graph: Cholera Case Numbers - This graph presents cholera case data over a normalized period (in years) with a fitted curve showing the estimated trend. Cholera cases have decreased significantly over time, as shown by the red fitted curve. This shows that initiatives, sanitation, clean water, and healthcare practices reduced cholera outbreaks over time. The bottom graph shows cholera deaths over the same time with observed data points and a fitted trend line. The fitted curve reveals a fall that matches the significant decline in deaths. This decline may be due to fewer instances, better treatment, response systems, and public health awareness throughout time.

Both graphs show cholera incidence and fatality declining, demonstrating public health efforts to control and prevent disease. The fitted curves illustrate that cholera remains a public health issue, but its impact has decreased over time.

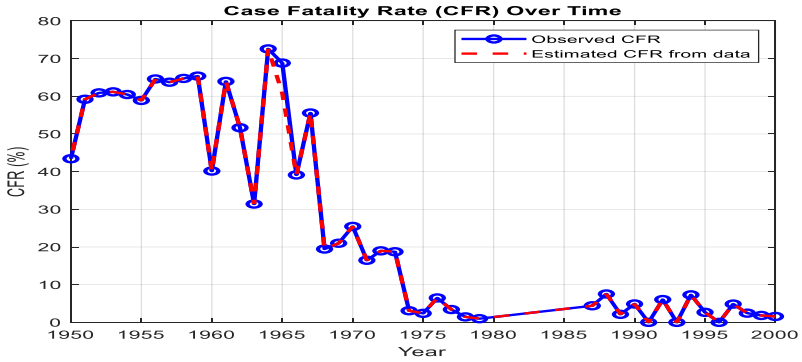

Fig. 5. Plot of the CFR over time

Figure 4, early CFR (1950s–1970s): High and variable. Early on, the CFR is high, ranging from 40% to 70%. This high prevalence shows cholera was a serious concern with few medical treatments. This may be owing to uneven medical care, ineffective treatment, or poor cholera management knowledge. The CFR begins to decrease sharply in the mid-1970s and reaches significantly lower levels by 1980. Cholera treatment breakthroughs like oral rehydration therapy (ORT), which reduces mortality by treating dehydration, the main cause, may have contributed to this period. The late 1980s to 2000: The CFR stabilizes at low levels, frequently under 10% and sometimes reaching 0%. This consistency shows that cholera management approaches grew more standardized and accessible due to improved public health infrastructure, awareness, and potential vaccine availability elsewhere. Estimating CFR with Curve-Fitting: The dashed red line shows a curve-fitting model applied to CFR data. This line smooths oscillations and calculates CFR's long-term trajectory. The fitted line matches the observed data points (blue circles) well, indicating that the model captures CFR decrease patterns. The second part of the 20th century saw a considerable decrease in cholera fatalities due to treatment and management advances. Improved healthcare interventions, access to appropriate treatments, and public health measures for cholera outbreaks reduced CFR.

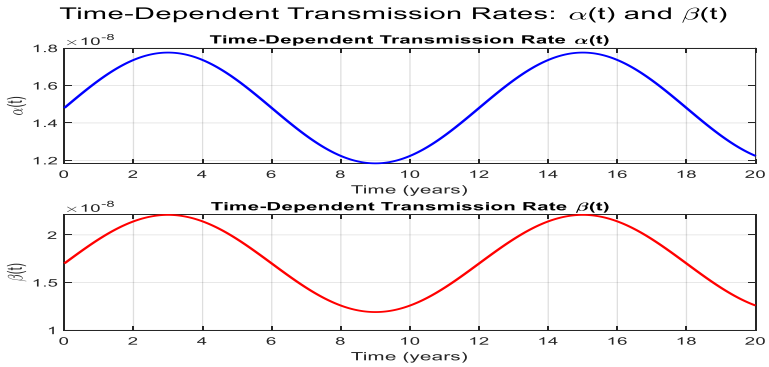

Fig. 6. Graph of the time-dependent rate for $\alpha(t)$ and $\beta(t)$

Graph - $\alpha(t)$: The graphs depict time-dependent transmission rates for parameters $\alpha(t)$ and $\beta(t)$ over 20 years, using a sinusoidal function to model seasonal or periodic variations in transmission. This graph shows the variation in the transmission rate $\alpha(t)$ as a function of time. It follows the equation:

$$\alpha(t) = \alpha_0\left(1 + A_\alpha sin\left(\frac{2\pi t}{T}\right)\right)$$

where α_0 is the base rate, A_α is the amplitude of seasonal variation, and T represents the period (assumed here to be one year). The oscillations indicate that the transmission rate increases and decreases periodically, reaching peaks and troughs that reflect potential seasonal influences on disease transmission or other environmental factors affecting $\alpha(t)$.

Graph - $\boldsymbol{\beta(t)}$: This graph shows the periodic behaviour of $\beta(t)$, following a similar sinusoidal form: $\beta(t) = \beta_0\left(1 + A_\beta sin\left(\frac{2\pi t}{T}\right)\right)$. Like $\alpha(t), \beta(t)$ oscillates, indicating fluctuations in the disease transmission parameter that could result from changes in social behavior, climate factors, or other time-dependent variables that impact the disease spread rate.

Both graphs illustrate how time-dependent functions can capture cyclical trends in transmission, which is valuable in epidemiological modeling to account for patterns such as seasonal peaks in infections. These periodic trends are often observed in diseases affected by environmental factors (e.g., rainfall for waterborne diseases) or human behaviors (e.g., increased contact rates during specific times of the year). This approach provides a more realistic representation of transmission dynamics than assuming constant rates.

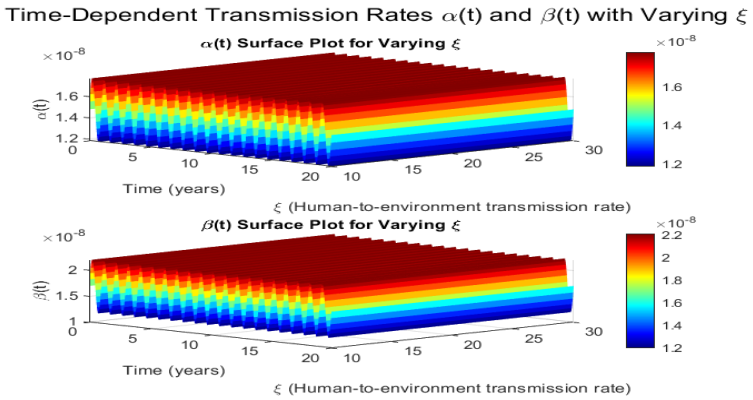

Fig. 7. Graph of the time-dependent rate for $\alpha(t)$ **and** $\beta(t)$ with varying ξ

The graphs depict the time-dependent transmission rates α(t) and β(t), which exhibit periodic fluctuations and are affected by the parameter ξ, denoting the human-to-environment transmission rate. The sinusoidal configuration of the curves along the temporal axis indicates a periodic or seasonal variation in transmission rates. This recurring pattern may be ascribed to seasonal variations, social behaviors, or environmental conditions influencing disease transmission rates. As ξ ascends along the y-axis, the extrema of α(t) and β(t) similarly rise. This suggests that increased human-to-environment transmission, or bacterial shedding, results in an escalation of these transmission rates. Consequently, when ξ is elevated, the peaks in α(t) and β(t) become more apparent, indicating a heightened risk of infection during periods of elevated transmission.

The colour gradient in the surface plots, transitioning from blue to red, visually signifies the intensity of α(t) and β(t). Lower values are shown in blue, and greater values are depicted in red. This gradient illustrates that as it increases, transmission rates escalate, resulting in heightened infection risks. These data highlight the necessity of regulating bacterial shedding in the environment, as it may alleviate transmission rate surges and hence diminish the incidence and intensity of outbreaks over time.

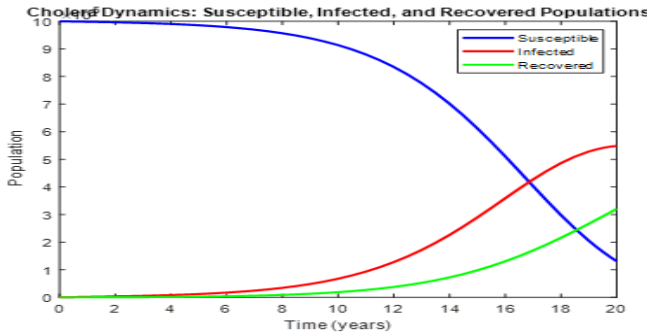

Fig. 8. Curve of the dynamics of the model

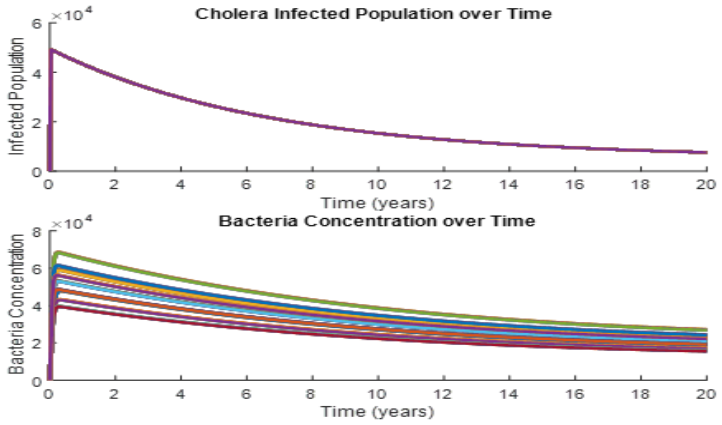

Fig. 9. Plot of infected population and bacteria concentrations

The reduction in the infected population remains consistently stable across a variety of parameter configurations, illustrating the model's robustness in capturing infection dynamics relative to bacterial growth and decay rates. Analysis of bacterial concentration trends reveals that environmental persistence and proliferation of *Vibrio cholerae* are highly sensitive to parameter changes. Specifically, elevated bacterial shedding rates (ξ), higher growth rates (r), and lower natural loss rates (w) contribute to an extended environmental presence of the pathogen, which could elevate the risk of sustained cholera transmission, especially in settings with favorable conditions for re-infection. Sensitivity analysis underscores the impact of these parameters, suggesting potential avenues for public health interventions. Targeted environmental sanitation efforts aimed at increasing bacterial decay rates (i.e., maximizing w) or vaccination campaigns to reduce host shedding rates (ξ) could substantially reduce the pathogen's environmental reservoir, thereby diminishing cholera's transmission potential. This model thus offers valuable insights into the interdependence of infection dynamics and environmental factors, facilitating strategic intervention planning to curb cholera's environmental prevalence and transmission.

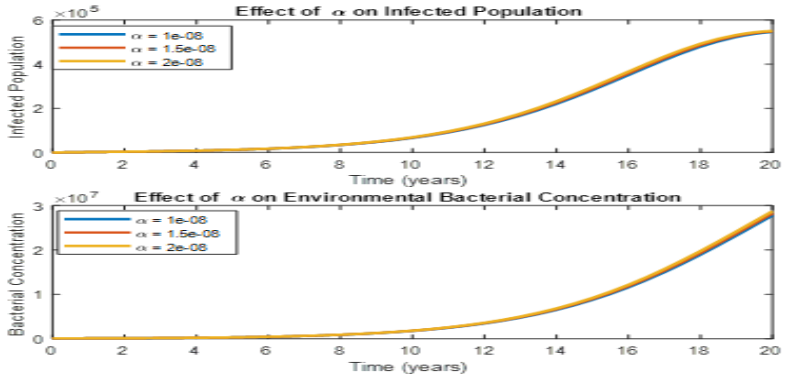

Fig. 10. Effect of β on infected bacteria concentration

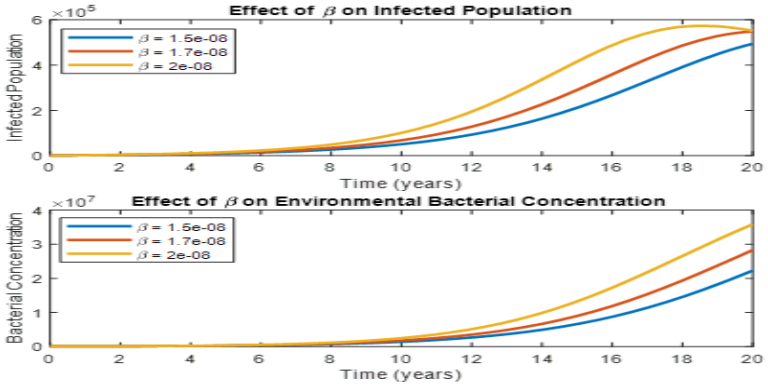

Fig. 11. Effect of β on infected bacteria concentration

Figure 9: The initial plot (top) illustrates the infected population over 20 years. Various values of β (1.5e-8, 1.7e-8, and 2e-8) yield distinct growth rates for the infected population. Elevated values of β result in a more rapid escalation in the population of infected individuals, as β denotes the rate at which susceptible individuals acquire infection from environmental influences. As β escalates, the transmission rate also increases, resulting in a more accelerated and significant expansion of the infected population. In the second plot (bottom), the bacterial concentration in the environment is observed to rise with time for each β value. A higher β results in a greater accumulation of germs in the environment, hence sustaining and enhancing the disease transmission cycle. Note that, augmenting the transmission rate β exerts a multiplicative influence on both the infected populace and bacterial concentration. This outcome highlights the necessity of regulating environmental conditions to mitigate disease outbreaks since minor changes in transmission rates can result in significantly elevated infection levels and environmental damage.

Figure 10: The graph above illustrates the effect of altering the baseline transmission rate represented on the dynamics of the infected population and bacterial concentration over 20 years. Three distinct values of α are utilized: $\alpha = 1 \times 10\text{^}\{-8\}$, $\alpha = 1.5 \times 10\text{^}\{-8\}$, and $\alpha = 2 \times 10\text{^}\{-8\}$.

The upper graph illustrates the temporal progression of the infected population, demonstrating that higher values of the transmission parameter α lead to a more rapid increase in the number of infected individuals. The parameter α represents the baseline transmission rate, and as it increases, the rate at which susceptible individuals are exposed to the disease accelerates, resulting in a more rapid spread of infection. For example, when α is elevated, the infected population reaches higher values in a shorter time, indicating a faster and more intense outbreak. This suggests that the disease spreads more efficiently, overwhelming the susceptible population and leading to a more pronounced epidemic.

Similarly, the lower plot depicting bacterial concentration shows a comparable upward trend. As α increases, the bacterial concentration in the environment rises

more rapidly and reaches higher levels. This is likely due to the correlation between the size of the infected population and the environmental bacterial load, as infected individuals contribute to bacterial shedding into the environment. With an elevated α, the disease spreads more quickly, increasing the number of infected individuals who subsequently release more bacteria, thus escalating the environmental concentration.

These findings underscore the interplay between transmission rates and both disease progression and environmental contamination. Elevated baseline transmission rates not only result in a more severe and accelerated epidemic but also significantly impact the environmental bacterial load, which can further facilitate the spread of the disease. This highlights the critical importance of managing and controlling transmission rates to mitigate the severity of cholera outbreaks and reduce their impact on public health. The model's insights can inform targeted intervention strategies aimed at slowing transmission and controlling bacterial contamination in affected areas. The colour gradient in the surface plots, transitioning from blue to red, visually signifies the intensity.

VI. Discussion of Results

The graphical juxtaposition of observed and estimated Case Fatality Rates (CFR) underscores the reliability and efficacy of the RK4 approach in precisely resolving the system of differential equations that form the basis of the model, This illustrates the method's efficacy in accurately capturing intricate dynamics. Here's a concise summary of that paragraph:

Extensive data preprocessing enhances model stability and clarity, including interpolation and smoothing. Unlike traditional models, the proposed approach incorporates variable recovery rates and environmental factors, offering a more realistic simulation of cholera dynamics. This comprehensive framework supports accurate epidemic modeling and informs effective public health measures and interventions. The strong correlation between the observed case fatality rate (CFR) and the calculated values suggests that the model effectively represents critical elements of disease progression and mortality risk, possibly serving as a dependable instrument for comprehending cholera dynamics. The model's incorporation of time-dependent transmission rates to account for seasonal variations is noteworthy. Seasonal fluctuations, presumably impacted by environmental factors like precipitation and temperature, influence cholera transmission via water sources and human interaction rates. This cyclical variation in transmission rates aids in replicating real-world situations, as cholera epidemics frequently surge during specific seasons due to conducive conditions for bacterial proliferation and dissemination. The results emphasize data-driven modeling in disease epidemiology. Our model is calibrated with historical data to better understand how diverse factors affect cholera patterns, helping public health officials prepare and respond to outbreaks. These findings show the model's potential for predicting cholera dynamics and assessing infection and fatality reduction measures. The parameters α, β, and ξ play critical roles in shaping the transmission dynamics of cholera, each influencing different aspects of the disease spread. Understanding their interactions and impact is essential for designing effective control strategies.

a) Human-to-Human Transmission Rate (α): This parameter quantifies the rate at which cholera is transmitted directly from infected individuals to susceptible individuals through contact. Variations in α can significantly alter the course of an epidemic. A higher α increases the likelihood of person-to-person transmission, which accelerates the spread of cholera, particularly in densely populated areas or regions with inadequate sanitation infrastructure. The rapid transmission observed in such environments underscores the importance of controlling this parameter. By improving sanitation, promoting hygiene practices, and enhancing public health awareness, α can be reduced, thereby curbing the rate of new infections. The model suggests that targeted interventions aimed at reducing α could significantly slow the disease's spread.

b) Environment-to-Human Transmission Rate (β): β represents the rate at which cholera is transmitted from contaminated environmental sources—primarily water—into humans. Given the waterborne nature of cholera, β is crucial for understanding seasonal fluctuations and outbreak risks. Environmental factors such as rainfall, flooding, and poor water management contribute to the dispersion and concentration of the Vibrio cholerae bacteria in the environment, thereby increasing β. During periods of heavy rainfall or flooding, β is likely to surge, leading to outbreaks. The model indicates that reducing β through improvements in water sanitation, infrastructure, and flood management could significantly decrease the frequency and severity of cholera outbreaks, particularly in regions with seasonal variability in environmental conditions.

c) Bacterial Growth Rate (ξ): The bacterial growth rate, ξ, dictates how rapidly cholera bacteria proliferate in the environment. A higher ξ corresponds to an increased concentration of bacteria in contaminated water sources, elevating the risk of transmission. Areas with inadequate sewage treatment or contaminated water bodies may experience elevated ξ, leading to higher bacterial loads and, consequently, a greater potential for human exposure. The model suggests that interventions aimed at reducing environmental contamination, such as improving waste management and treating drinking water, could lower ξ, thereby decreasing the likelihood of environmental transmission. This would directly reduce the number of infections originating from contaminated water sources.

Together, the interplay of α, β, and ξ underscores the need for a multifaceted approach to cholera control. Targeted interventions aimed at improving water quality, sanitation, and reducing direct human-to-human contact during outbreaks can effectively manage the disease’s transmission. The model's sensitivity to these parameters highlights the importance of adaptive strategies that account for seasonal changes, environmental conditions, and public health dynamics. Continuous monitoring and timely interventions, tailored to the local context, are essential for long-term cholera control and prevention.

VII. Conclusions

The application of the RK4 method in the model highlights its effectiveness in solving differential equations with accuracy and stability. It successfully captures complex interactions and parameter variations, making it a robust tool for simulating cholera dynamics and analyzing epidemiological trends. In conclusion, the study highlights the critical influence of human-to-human α and environment-to-human β transmission rates and the bacterial growth rate ξ in shaping cholera dynamics. Through modeling and parameter estimation, it is evident that reducing these factors through public health interventions such as improved sanitation, access to clean water, and timely treatment can significantly curtail cholera outbreaks. The findings underscore the importance of targeting environmental factors and seasonal transmission patterns to achieve sustainable control and prevention of cholera. Future efforts should focus on integrating these strategies into public health policies for enhanced epidemic management.

VIII. Acknowledgement

This research is supported by Universiti Sains Malaysia and Phuket Rajabhat University under the Visiting Scholar Program.

Conflict of Interest:

There was no relevant conflict of interest regarding this paper.

References

I. Al-Tawfiq, J. A., Chopra, H., Dhama, K., Sah, R., Schlagenhauf, P., & Memish, Z. A. (2022). The Cholera Challenge: How Should the World Respond? *New Microbes and New Infections*, *51*, 101077. 10.1016/j.nmni.2022.101077

II. Ayoade, A. A., Ibrahim MO, Peter OJ, and F. A. Oguntolu. "A mathematical model on cholera dynamics with prevention and control." *Covenant Journal of Physical and Life Sciences* (2018). https://journals.covenantuniversity.edu.ng/index.php/cjpls/article/view/933

III. Brhane, Kewani Welay, et al. "Mathematical modelling of cholera dynamics with intrinsic growth considering constant interventions." *Scientific Reports* 14.1 (2024): 4616. 10.1038/s41598-024-55240-0

IV. Cirri, Emilio, and Georg Pohnert. "Algae-bacteria interactions that balance the planktonic microbiome." *New Phytologist* 223.1 (2019): 100-106. 10.1111/nph.15765

V. Emmanuel, Sabastine, et al. "Population Growth Forecasting Using the Verhulst Logistic Model and Numerical Techniques." *Intelligent Systems Modeling and Simulation III: Artificial Intelligent, Machine Learning, Intelligent Functions and Cyber Security*. Cham: Springer Nature Switzerland, 2024. 191-202. https://link.springer.com/chapter/10.1007/978-3-031-67317-7_12.

VI. Ezeagu, Nneamaka Judith, Houénafa Alain Togbenon, and Edwin Moyo. "Modelling and analysis of cholera dynamics with vaccination." *American Journal of Applied Mathematics and Statistics* 7.1 (2019): 1-8. 10.12691/ajams-7-1-1

VII. Ghosh, Ahona, Sandip Roy, Haraprasad Mondal, Suparna Biswas, and Rajesh Bose. "Mathematical modelling for decision making of lockdown during COVID-19." *Applied Intelligence* 52.1 (2022): 699-715. 10.1007/s10489-021-02463-7

VIII. Hailemariam Hntsa, Kinfe, and Berhe Nerea Kahsay. "Analysis of cholera epidemic control using mathematical modelling." *International Journal of Mathematics and Mathematical Sciences* 2020.1 (2020): 7369204. 10.1155/2020/7369204

IX. Ilic, Irena, and Milena Ilic. "Global patterns of trends in cholera mortality." *Tropical Medicine and Infectious Disease* 8.3 (2023): 169. 10.3390/tropicalmed8030169

X. Kolaye, G. G., et al. "Mathematical assessment of the role of environmental factors on the dynamical transmission of cholera." *Communications in Nonlinear Science and Numerical Simulation* 67 (2019): 203-222. 10.1016/j.cnsns.2018.06.023

XI. Marques, Lara, et al. "Advancing precision medicine: a review of innovative in silico approaches for drug development, clinical pharmacology and personalised healthcare." *Pharmaceutics* 16.3 (2024): 332. 10.3390/pharmaceutics16030332

XII. Onitilo, Sefiu et al. “Modelling the Transmission Dynamics of Cholera Disease With the Impact of Control Strategies in Nigeria”. Cankaya University Journal of Science and Engineering, vol. 20, no. 1, 2023, pp. 35-52. https://dergipark.org.tr/en/download/article-file/3015343

XIII. Onuorah, Martins O., F. A. Atiku, and H. Juuko. "Mathematical model for prevention and control of cholera transmission in a variable population." *Research in Mathematics* 9.1 (2022): 2018779. 10.1080/27658449.2021.2018779

XIV. Orishaba, Philip, et al. "Cholera epidemic amidst the COVID-19 pandemic in Moroto district, Uganda: Hurdles and opportunities for control." *PLOS global public health* 2.10 (2022): e0000590. 10.1371/journal.pgph.0000590

XV. Rashid, Saima, Fahd Jarad, and Abdulaziz Khalid Alsharidi. "Numerical investigation of fractional-order cholera epidemic model with transmission dynamics via fractal–fractional operator technique." *Chaos, Solitons & Fractals* 162 (2022): 112477. 10.1016/j.chaos.2022.112477

XVI. Ravindra, Khaiwal, Nitasha Vig, Kalzang Chhoden, Ravikant Singh, Kaushal Kishor, Nityanand Singh Maurya, Shweta Narayan, and Suman Mor. "Impact of massive flood on drinking water quality and community health risk assessment in Patna, Bihar, India." *Sustainable Water Resources Management* 10.3 (2024): 104. 10.1007/s40899-024-01052-z

XVII. Shannon, Kerry, Marisa Hast, Andrew S. Azman, Dominique Legros, Heather McKay, and Justin Lessler. "Cholera prevention and control in refugee settings: successes and continued challenges." *PLoS neglected tropical diseases* 13.6 (2019): e0007347. 10.1371/journal.pntd.0007347

XVIII. Tilahun, Getachew Teshome, Woldegebriel Assefa Woldegerima, and Aychew Wondifraw. "Stochastic and deterministic mathematical model of cholera disease dynamics with direct transmission." *Advances in Difference Equations* 2020.1 (2020): 670. 10.1186/s13662-020-03130-w

XIX. Vandendriessche, Joris. "Cholera, corona and trust in numbers." *Journal for the History of Environment and Society* 5 (2021): 47-52. https://lirias.kuleuven.be/retrieve/674683

XX. Wang, Wei, and Zhaosheng Feng. "Influence of environmental pollution on a waterborne pathogen model: Global dynamics and asymptotic profiles." *Communications in Nonlinear Science and Numerical Simulation* 99 (2021): 105821. 10.1016/j.cnsns.2021.105821

XXI. Yang, Chayu, and Jin Wang. "On the intrinsic dynamics of bacteria in waterborne infections." *Mathematical Biosciences* 296 (2018): 71-81. 10.1016/j.mbs.2017.12.005